(Fig. 2). NLRP3 activation in monocytes results in elevated serum IL-1β level, while its activation and IL-1β secretion by dermal mast cells are associated with vascular leakage and neutrophil recruitment in the urticarial rash.[41]

Anti–IL-1 therapies, including recombinant IL-1 receptor antagonist (IL-1Ra) known as anakinra, rilonacept, composed of extracellular IL-1RI and accessory protein (AcP), and anti–IL-1β antibodies such as canakinumab, dramatically improve almost all symptoms of CAPS, indicating the critical role played by IL-1β in the development of CAPS.[42–44]

NAPS12

Two unrelated families with an autosomal dominantly inherited periodic fever syndrome were reported from Guadeloupe in 2008.[5] In one family, twin sons and their father were affected. The sons showed episodic fever, arthralgia, and myalgia induced by generalized cold exposure since the first days of life. Urticaria was also observed twice in each patient. Headache and lower limb pain occurred during and between episodes, and both patients had bilateral sensorineural hearing loss. Their father had also experienced occasional attacks during childhood and still showed episodes of fever and urticaria triggered by physical activities, without hearing loss. An affected daughter in the second family developed cold-induced episodic fever with abdominal pain, vomiting, arthralgia, buccal aphthous ulcers, and lymphadenopathy since the
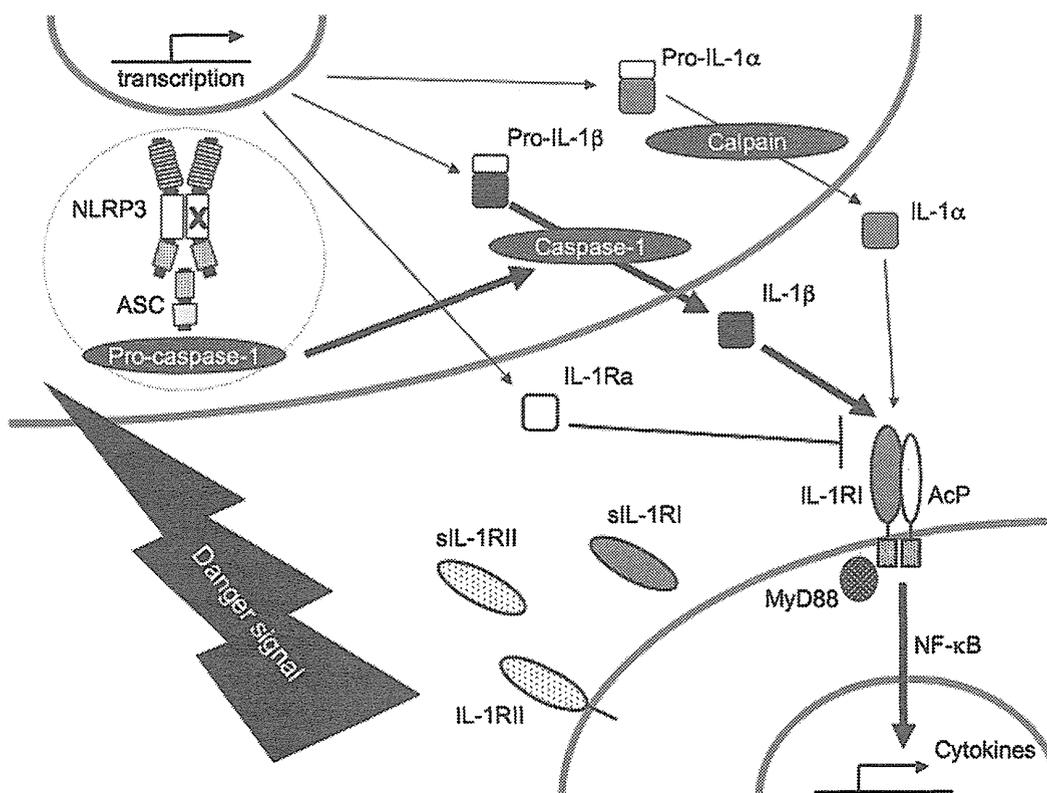
Fig. 2. Molecular pathogenesis of CAPS. In CAPS, a heterozygous *NLRP3* mutation (indicated by X in dimerized molecules) causes constitutive activation of the inflammasome complex (surrounded by a broken-lined circle), leading to cleavage of preformed pro-IL-1β with activated caspase-1 and secretion of mature IL-1β to cause sustained inflammation. On danger, only one signal to induce transcription of pro-IL-1β mRNA is enough for secretion of mature IL-1β. The decoy receptor IL-1RII, soluble (s) IL-1RI and sIL-1RII, as well as IL-1Ra, are all negative regulators of IL-1 signaling.

first year of life. Her affected father also had attacks with fever and abdominal pain between the ages of 5 and 12 years.

Because of the similarity of their symptoms to CAPS, their disease was designated as FCAS2 (OMIM #611762). Through an extensive search for mutations in NLR family molecules, heterozygous nonsense or insertion mutations in the *NLRP12* gene have been identified in each family.[5] A base-pair insertion within the donor splice site of intron 3 activates a cryptic donor splice site, resulting in a frame shift and a premature termination. As NLRP12 has been shown to be a negative regulator of nuclear factor (NF)-κB signaling and such an inhibitory effect was actually impaired by these mutations, their heterozygosity seems to cause haploinsufficiency in patients.[45]

PLAID

Three unrelated families with autosomal dominantly inherited atypical cold urticaria were first reported in 2009.[46] As a characteristic feature, water evaporation seems to be the most effective stimulus, which is occasionally induced by tears flowing down the cheeks or warm water on the skin exposed to room temperature. Accordingly, the patients show a negative cold-stimulation test using ice cubes, whereas urticarial rashes appear after direct contact of ice to the skin followed by rewarming to room temperature. Outdoor cold air also induces urticarial rash over unprotected areas. All patients experienced pruritus and erythema, whereas angioedema was experienced by less than half of the cases. Reactions are local rather than generalized, are not accompanied by systemic complications, and usually resolve within 30 minutes. Of note, ingestion of cold foods or beverages caused oropharyngeal swelling in some cases. Most patients develop the symptoms before 6 months of age and sustain them for life, although their severity usually improves after 30 years of age. The disease has been designated as familial atypical cold urticaria (FACU) or FCAS3 (OMIM #614468), which is clearly distinguished from FCAS by the absence of systemic involvement.

In 2012, immunologic abnormalities were added to their clinical features. These abnormalities include recurrent infections associated with low immunoglobulin (Ig)A and IgM, and high IgE levels in the serum, decreased circulating B cells and natural killer (NK) cells, and development of autoantibodies or autoimmune diseases and granulomatous skin lesions.[6] Through linkage analysis, 3 different heterozygous deletions in the *PLCG2* gene have been identified as responsible, and the disease has been designated as PLAID. Phospholipase C (PLC) family enzymes hydrolyze membranous phospholipids and generate diacylglycerols and inositol triphosphate to activate calcium influx. Among them, PLCγ2 is expressed in B, NK, and mast cells, and involves signaling through various receptor tyrosine kinases. All 3 deletions are included in the C-terminal Src-homology-2 (SH2) domain with an autoinhibitory role, and lack of this domain has been shown to increase the phospholipase activity of PLCγ2. The downstream functions of the immune cells, however, were mostly decreased, probably as a result of chronic signaling. By contrast, mast cells with mutant *PLCG2* showed spontaneous degranulation at 20°C, probably responsible for cold urticaria.[6]

Almost simultaneously, familial cases showing recurrent blistering skin lesions with inflammatory lesions of the joints, eyes, and gastrointestinal tract were reported.[7] Their skin lesions resembled epidermolysis bullosa in infancy, but progressed to erythematous plaques with vesiculopustules, which worsened with heat and sun exposure. These patients also showed mild deficiency of humoral immunity causing recurrent sinopulmonary infections, without circulating autoantibodies. Through whole exome sequencing, a heterozygous gain-of-function missense mutation in the *PLCG2*

Table 4
Hereditary diseases with cold-induced urticaria

		Episodic Symptoms	Sustained/Progressive Symptoms
CAPS	FCAS	Urticarial rash, arthralgia, myalgia, chills, fever, swelling of the extremities	Renal amyloidosis
	MWS	Urticarial rash, arthralgia, chills, fever	Sensorineural deafness, renal amyloidosis
	CINCA	Fever	Rash, arthritis, chronic meningitis, visual defect, deafness, growth retardation, renal amyloidosis
NAPS12 (FCAS2)		Fever, arthralgia, myalgia, urticaria, abdominal pain, aphthous ulcers, lymphadenopathy	Sensorineural deafness
PLAID (FCAS3)		Urticaria induced by evaporative cooling, sinopulmonary infections	Serum low immunoglobulin (Ig)M and IgA levels, high IgE levels, decreased B and NK cells, granulomata, antinuclear antibodies

gene has been identified as being responsible.[7] Despite some distinctive clinical and genetic features, the diseases in this family and the families with PLAID possibly form a distinct type of hereditary autoinflammatory syndrome with immunodeficiency. The clinical features of hereditary diseases with cold-induced urticaria are summarized in Table 4.

OTHER GENETICALLY UNDEFINED HEREDITARY URTICARIA

On searching the OMIM database, several disorders with distinct OMIM numbers remain to be genetically defined. Aquagenic urticaria (OMIM 191850) is characterized by urticaria induced by contact with water but not by heat or cold, and its familial occurrence was reported in 1979.[47] Familial cases with delayed heat urticaria were reported as familial localized heat urticaria (OMIM 191950),[48] in which the lesions were limited to the areas of contact with heat and were completely inhibited by local lidocaine pretreatment. Another 2 forms of familial physical urticaria, dermodistortive urticaria (OMIM 125630) and familial dermographism (OMIM 125635), are also registered.[49,50] The former is induced by repetitive vibratory or stretching stimulation, whereas the latter is defined by wheal formation on the skin after a single stroke with moderate pressure.

SUMMARY

Hereditary disorders presenting with urticaria are not common and may not be encountered by most physicians. However, without the correct knowledge they can be easily missed or misdiagnosed. With proper diagnosis and understanding of the genetic cause and consequent pathogenesis, disease-specific essential therapeutic regimens can be offered. Recent discovery of the genetic origins of rare cases with distinct hereditary cold urticaria encourages the examination of more cases. As technology in genetic analysis progresses rapidly, further insights into undefined hereditary urticaria will emerge in the near future. The knowledge obtained promises to lead to the development of novel therapeutics.

REFERENCES

1. Hide M, Hiragun T. Japanese guidelines for diagnosis and treatment of urticaria in comparison with other countries. Allergol Int 2012;61:517–27.
2. Fuller SJ. New insights into the pathogenesis, diagnosis, and management of mastocytosis. Hematol Oncol Clin North Am 2012;26:1143–68.
3. Cicardi M, Johnston DT. Hereditary and acquired complement component 1 esterase inhibitor deficiency: a review for the hematologist. Acta Haematol 2012;127:208–20.
4. Yu JR, Leslie KS. Cryopyrin-associated periodic syndrome: an update on diagnosis and treatment response. Curr Allergy Asthma Rep 2011;22:12–20.
5. Jeru I, Duquesnoy P, Fernandes-Alnemri T, et al. Mutations in NALP12 cause hereditary periodic fever syndromes. Proc Natl Acad Sci U S A 2008;105:1614–9.
6. Ombrello MJ, Remmers EF, Sun G, et al. Cold urticaria, immunodeficiency, and autoimmunity related to PLCG2 deletions. N Engl J Med 2012;366:330–8.
7. Zhou Q, Lee GS, Brady J, et al. A hypermorphic missense mutation in PLCG2, encoding phospholipase Cγ2, causes a dominantly inherited autoinflammatory disease with immunodeficiency. Am J Hum Genet 2012;91:713–20.
8. Kettelhut BV, Metcalfe DD. Pediatric mastocytosis. J Invest Dermatol 1991;96: 15S–8S.
9. Middelkamp Hup MA, Heide R, Tank B, et al. Comparison of mastocytosis with onset in children and adults. J Eur Acad Dermatol Venereol 2002;16:115–20.
10. Topar G, Staudacher C, Geisen F, et al. Urticaria pigmentosa: a clinical, hematopathologic, and serologic study of 30 adults. Am J Clin Pathol 1998;109: 279–85.
11. Wolff K, Komr M, Petzelbauer P. Clinical and histopathological aspects of cutaneous mastocytosis. Leuk Res 2001;25:519–28.
12. Golitz LE, Weston WL, Lane AT. Bullous mastocytosis: diffuse cutaneous mastocytosis with extensive blisters mimicking scalded skin syndrome or erythema multiforme. Pediatr Dermatol 1984;1:288–94.
13. Horny HP, Parwaresch MR, Lennert K. Bone marrow findings in systemic mastocytosis. Hum Pathol 1985;16:808–14.
14. Longley BJ, Metcalfe DD, Tharp M, et al. Activating and dominant inactivating c-KIT catalytic domain mutations in distinct clinical forms of human mastocytosis. Proc Natl Acad Sci U S A 1999;96:1609–14.
15. Bodemer C, Hermine O, Palmerini F, et al. Pediatric mastocytosis is a clonal disease associated with D816V and other activating c-KIT mutations. J Invest Dermatol 2010;130:804–15.
16. Garcia-Montero AC, Jara-Acevedo M, Teodosio C, et al. KIT mutation in mast cells and other bone marrow hematopoietic cell lineages in systemic mast cell disorders: a prospective study of the Spanish Network on Mastocytosis (REMA) in a series of 113 patients. Blood 2006;108:2366–72.
17. Fett NM, Teng J, Longley BJ. Familial urticarial pigmentosa: report of a family and review of the role of KIT mutations. Am J Dermatopathol 2013;35:113–6.
18. Gleixner KV, Mayerhofer M, Ceyny-Reiterer S, et al. KIT-D816V-independent oncogenic signaling in neoplastic cells in systemic mastocytosis: role of Lyn and Btk activation and disruption by dasatinib and bosutinib. Blood 2011;118: 1885–98.
19. Yanagihori H, Oyama N, Nakamura K, et al. c-KIT Mutations in patients with childhood-onset mastocytosis and genotype-phenotype correlation. J Mol Diagn 2005;7:252–7.

20. Shaw JM. Genetic aspects of urticaria pigmentosa. Arch Dermatol 1968;97: 137–8.

21. Wasag B, Niedoszytko M, Piskorz A, et al. Novel, activating KIT-N822I mutation in familial cutaneous mastocytosis. Exp Hematol 2011;39:859–65.

22. Quincke HI. Uber akutes umschriebenes Hautoderm. Monatsh Prakt Derm 1882;1:129–31.

23. Donaldson VH, Evans RR. A biochemical abnormality in hereditary angioneurotic edema: absence of serum inhibitor of C'1-esterase. Am J Med 1963;35:37–44.

24. Lumry WR, Castaldo AJ, Vernon MK, et al. The humanistic burden of hereditary angioedema: impact on health-related quality of life, productivity, and depression. Allergy Asthma Proc 2010;31:407–14.

25. Nzeako UC, Frigas E, Tremaine WJ. Hereditary angioedema: a broad review for clinicians. Arch Intern Med 2001;161:2417–29.

26. Bork K, Barnstedt SE, Koch P, et al. Hereditary angioedema with normal C1-inhibitor activity in woman. Lancet 2000;356:213–7.

27. Dewald G, Bork K. Missense mutations in the coagulation factor XII (Hageman factor) gene in hereditary angioedema with normal C1 inhibitor. Biochem Biophys Res Commun 2006;343:1286–9.

28. Cichon S, Martin L, Hennies HC, et al. Increased activity of coagulation factor XII (Hageman factor) causes hereditary angioedema type III. Am J Hum Genet 2006;79:1098–104.

29. Nussberger J, Cugno M, Amstutz C, et al. Plasma bradykinin in angio-oedema. Lancet 1998;351:1693–7.

30. Bowen T, Cicardi M, Farkas H, et al. 2010 international consensus algorithm for the diagnosis, therapy and management of hereditary angioedema. Allergy Asthma Clin Immunol 2010;6:24.

31. Kile RL, Rusk HA. A case of cold urticaria with unusual family history. JAMA 1940;114:1067–8.

32. Muckle TJ, Wells M. Urticaria, deafness and amyloidosis: a new heredo-familial syndrome. Q J Med 1962;31:235–48.

33. Hoffman HM, Mueller JL, Broide DH, et al. Mutation of a new gene encoding a putative pyrin-like protein causes familial cold autoinflammatory syndrome and Muckle-Wells syndrome. Nat Genet 2001;29:301–5.

34. Kastner DL, O'Shea JJ. A fever gene comes in from the cold. Nat Genet 2001; 29:241–2.

35. Feldmann J, Prieur AM, Quartier P, et al. Chronic infantile neurological cutaneous and articular syndrome is caused by mutations in CIAS1, a gene highly expressed in polymorphonuclear cells and chondrocytes. Am J Hum Genet 2002;71:198–203.

36. Aksentijevich I, Nowak M, Mallah M, et al. De novo CIAS1 mutations, cytokine activation, and evidence for genetic heterogeneity in patients with neonatal-onset multisystem inflammatory disease (NOMID): a new member of the expanding family of pyrin-associated autoinflammatory diseases. Arthritis Rheum 2002;46:3340–8.

37. Arostegui JI, Aldea A, Modesto C, et al. Clinical and genetic heterogeneity among Spanish patients with recurrent autoinflammatory syndromes associated with the CIAS1/PYPAF1/NALP3 gene. Arthritis Rheum 2004;50:4045–50.

38. Tanaka N, Izawa K, Saito MK, et al. High incidence of NLRP3 somatic mosaicism in patients with chronic infantile neurologic, cutaneous, articular syndrome: results of an international multicenter collaborative study. Arthritis Rheum 2011; 63:3625–32.

39. Kersse K, Bertrand MJ, Lamkanfi M, et al. NOD-like receptors and the innate immune system: coping with danger, damage and death. Cytokine Growth Factor Rev 2011;22:257–76.

40. McDermott MF, Tschopp J. From inflammasomes to fevers, crystals and hypertension: how basic research explains inflammatory diseases. Trends Mol Med 2007;13:381–8.

41. Nakamura Y, Kambe N, Saito M, et al. Mast cells mediate neutrophil recruitment and vascular leakage through the NLRP3 inflammasome in histamine-independent urticaria. J Exp Med 2009;206:1037–46.

42. Hoffman HM, Rosengren S, Boyle DL, et al. Prevention of cold-associated acute inflammation in familial cold autoinflammatory syndrome by interleukin-1 receptor antagonist. Lancet 2004;364:1779–85.

43. Hoffman HM, Throne ML, Amar NJ, et al. Efficacy and safety of rilonacept (interleukin-1 Trap) in patients with cryopyrin-associated periodic syndromes: results from two sequential placebo-controlled studies. Arthritis Rheum 2008;58: 2443–52.

44. Lachmann HJ, Kone-Paut I, Kuemmerle-Deschner JB, et al, Canakinumab in CAPS Study Group. Use of canakinumab in the cryopyrin-associated periodic syndrome. N Engl J Med 2009;360:2416–25.

45. Lich JD, Ting JP. Monarch-1/pypaf7 and other CATERPILLER (CLR, NOD, NLR) proteins with negative regulatory functions. Microbes Infect 2007;9:672–6.

46. Gandhi C, Healy C, Wanderer AA, et al. Familial atypical cold urticaria: description of a new hereditary disease. J Allergy Clin Immunol 2009;124:1245–50.

47. Bonnetblanc JM, Andrieu-Pfahl F, Meraud JP, et al. Familial aquagenic urticaria. Dermatologica 1979;158:468–70.

48. Michaelsson G, Ros AM. Familial localized heat urticaria of delayed type. Acta Derm Venereol 1971;51:279–83.

49. Epstein PA, Kidd KK. Dermo-distortive urticaria: an autosomal dominant dermatologic disorder. Am J Med Genet 1981;9:307–15.

50. Jedele KB, Michels VV. Familial dermographism. Am J Med Genet 1991;39: 201–3.

Ultrasonographic assessment reveals detailed distribution of synovial inflammation in Blau syndrome

Kei Ikeda[1*], Naotomo Kambe[2], Syuji Takei[3,4], Taiji Nakano[5], Yuzaburo Inoue[5], Minako Tomiita[6], Natsuko Oyake[7], Takashi Satoh[2], Tsuyoshi Yamatou[3], Tomohiro Kubota[3], Ikuo Okafuji[8], Nobuo Kanazawa[9], Ryuta Nishikomori[10], Naoki Shimojo[5], Hiroyuki Matsue[2] and Hiroshi Nakajima[1]

Abstract

Introduction: Arthritis is the most frequent manifestation of Blau syndrome, an autoinflammatory disorder caused by the genetic mutation of *NOD2*. However, detailed information on arthritis in Blau syndrome on which the therapeutic strategy should be based on is lacking. This multi-center study aimed to accurately characterize the articular manifestation of Blau syndrome and also to demonstrate the utility of musculoskeletal ultrasound in Blau syndrome.

Methods: Patients who had been diagnosed with Blau syndrome by genetic analysis of *NOD2* were recruited. A total of 102 synovial sites in 40 joints were assessed semiquantitatively by ultrasound for gray-scale synovitis and synovial power Doppler (PD) signal.

Results: In total, 10 patients whose age ranged from 10 months to 37 years enrolled in this study. Although only 4 joints (0.8%) were tender on physical examination, 81 joints (16.9%) were clinically swollen. Moreover, 240 (50.0%), and 124 (25.8%) joints showed gray-scale (GS) synovitis and synovial PD signal on ultrasound, respectively. Importantly, GS synovitis was present in 168 out of 399 non-swollen joints, in which 61 also exhibited synovial PD signal. Among 40 joint regions, the ankle, the wrist, and the proximal interphalangeal joints were the most frequently and severely affected joints. Comparisons between different synovial tissues demonstrated a significantly higher proportion of the joints with tenosynovitis as compared with that with intra-articular synovitis (41.5% versus 27.9%, $P < 0.0001$). In respect of age and treatment, synovial PD signals were minimal in the youngest patient and in the oldest two patients, and were relatively mild in patients receiving treatment with methotrexate plus TNF antagonists. In two patients who underwent the second ultrasound examination, total PD scores markedly decreased after initiating the treatment with a tumor necrosis factor (TNF) antagonist.

Conclusions: The detailed information on synovial inflammation obtained by ultrasound confirms the dissociation between pain and inflammation and the frequently involved joint regions and synovial tissue in the arthritis of Blau syndrome. Our data also demonstrate that ultrasonography can be a potent tool in monitoring the activity of synovial inflammation and in investigating the pathophysiology of arthritis in this rare but archetypical autoinflammatory condition.

* Correspondence: K.Ikeda@faculty.chiba-u.jp
[1]Department of Allergy and Clinical Immunology, Chiba University Hospital,
1-8-1 Inohana, Chuo-ku, Chiba 260-8677, Japan
Full list of author information is available at the end of the article

Introduction

Blau syndrome (MIM #186580) is a rare autoinflammatory disorder, which was first described in 1985 by the pediatrician Edward Blau as a dominantly inherited, chronic inflammatory syndrome characterized by the clinical triad of granulomatous dermatitis, symmetric arthritis and recurrent uveitis [1]. In 2001, Miceli-Richard *et al.* identified the gene that confers susceptibility for Blau syndrome, discovering three mis-sense mutations (R334Q, R334W and L469F) in the region encoding the nucleotide-binding oligomerization domain (NOD) of the caspase recruitment domain gene (*CARD15/NOD2*) in four French and German affected families [2]. In spite of the striking clinical similarities with Blau syndrome, early onset sarcoidosis (EOS, MIM #609464) was originally considered a distinct disease entity. However, subsequent genetic analyses have shown that many patients with EOS have mutations in *NOD2* [3-6] and these two diseases and other variant forms are now considered to represent a pathophysiologically identical condition in which increased NFκB activity driven by mutated *NOD2* gene plays a significant role [3,6-11].

Arthritis is the most frequent manifestation of Blau syndrome and usually becomes clinically apparent within the first decade of life [1,5,7,11-15]. Joint manifestation in Blau syndrome has been reported to be chronic, symmetrical, and mostly painless polyarthritis. Marked soft-tissue swelling can occur due to granulomatous inflammation in both intra-articular synovium and tenosynovium, which can cause characteristic camptodactyly (that is, flexion contracture of fingers and toes) and, occasionally, subsequent impairment of physical function. However, the precise location and severity of joint inflammation in patients with Blau syndrome have not been systematically evaluated because of the difficulty to accurately determine with physical examination the activity of current inflammation in mostly non-tender joints in children.

Musculoskeletal ultrasound is a relatively inexpensive imaging modality, which enables more accurate assessment of synovial inflammation than physical examination does [16-19] and, therefore, provides improved accuracy in the diagnosis [20-24] and the disease activity monitoring [19,23-29] of rheumatoid arthritis (RA). As ultrasound is a non-invasive technique, which patients can undergo with minimal restriction, its use in pediatric inflammatory conditions such as juvenile idiopathic arthritis (JIA) has been increasingly studied [30-33]. We recently reported representative ultrasound images that clearly visualized the tenosynovitis in a patient with Blau syndrome [34]; however, no other papers have reported the use of ultrasound in the assessment of synovial inflammation in Blau syndrome.

In this pilot, multicenter study, 10 patients with Blau syndrome whose *NOD2* mutation had been confirmed underwent comprehensive ultrasound examination of 102 synovial sites, aiming to accurately characterize the articular manifestation of Blau syndrome and also to demonstrate the utility of musculoskeletal ultrasound in Blau syndrome.

Patients and methods

Patients and NOD2 mutation analysis

In this cross-sectional study, patients who had been diagnosed with Blau syndrome by genetic analysis of *NOD2* were recruited. Age- and sex-matched control subjects who did not have arthritic symptoms were also recruited. Written informed consent was obtained from the patient/subject, or his/her family member if necessary, according to the study protocol approved by the Ethics Committee of Chiba University, Kyoto University, and Kagoshima University in accordance with the Declaration of Helsinki. Genomic DNA was extracted from the peripheral blood of the patients, and sequencing of all exons and exon-intron junctions of *NOD2* was performed as previously described [6].

Clinical and laboratory assessment

Clinical information collected was complete medical history including current and previous medication for Blau syndrome, tender and swollen joint counts in 40 joints (disease activity score in 28 joints (DAS28) + bilateral ankle and metatarsophalangeal (MTP) joints), patient's/parent's and physician's global visual analogue scale (VAS), erythrocyte sedimentation rate (ESR), serum levels of C-reactive protein (CRP) and matrix metalloproteinase-3 (MMP-3), childhood health assessment questionnaire-disability index (CHAQ-DI), and the presence of camptodactyly in fingers and toes.

Ultrasound examination

A systematic multiplanar gray-scale (GS) and power Doppler (PD) ultrasound was performed in a temperature-controlled room on the same day of the clinical evaluation by a rheumatologist who was experienced in musculoskeletal ultrasound (KI) using an HI VISION Ascendus with a linear array multi-frequency transducer (5 to 18 MHz for GS, 7.5 MHz for PD) (Hitachi Medical Corporation, Tokyo, Japan). PD ultrasound was performed with a pulse repetition frequency set at 800 Hz and a low wall filter. Color gain was set just below the level at which color noise appeared.

Ultrasound was performed on the 40 joints which were clinically assessed for joint counts. Middle and large joints were divided into individual joints which compose the larger joint unit (for example, humeroradial and humeroulnar joints in the elbow) or into multiple parts of the joint (for example, suprapatellar recess, medial and lateral aspects of femorotibial joints in the

knee) and a total of 54 intra-articular synovial sites were separately evaluated (Figure 1). In addition to the intra-articular synovium, we also evaluated the major peri-articular synovial tissues; a total of 44 tenosynovial sites (Figure 2) and 4 bursal sites (bilateral sub-acromial/del-toid bursae) were examined. All sites were scanned thoroughly in multiple imaging planes so that the whole lesion was evaluated. As no ultrasound definitions of synovial pathology have been established for children, we based our assessment on the ultrasound definitions

for adults [35]. However, particularly careful attention was paid in children to distinguishing unossified cartilage and its feeding blood vessels from true synovial pathology. As no ultrasound scoring system for synovial pathology in children has been established either, severity of synovial pathology in the 102 sites was graded subjectively utilizing the rater's experience in the clinical studies in adults [19,22,29,36-38]. Synovial hypertrophy and synovial fluid were graded as a GS score altogether on a scale of 0 to 3 (grade 0, normal; grade 1, mild; grade

Figure 1 Ultrasound scores for intra-articular synovitis in patients with Blau syndrome. Semiquantitative grades (0 to 3) for gray-scale synovitis and synovial power Doppler signal in individual joint regions are shown in heat maps. Total sum of the scores in each case is shown in the right column. *First ultrasound examination (before treatment); **second ultrasound examination (after treatment). GS, gray-scale; PD, power Doppler; No, case number; R, right; L, left; Ext, extensor; Lat, lateral; Post, posterior; Med, medial; PIP (IP), proximal interphalangeal (interphalangeal); MCP, metacarpophalangeal; RC, radiocarpal; IC, intercarpal; DRU, distal radioulnar; HR, humeroradial; HU, humeroulnar; GH, glenohumeral; SPR, suprapatellar recess; FT, femorotibial; TT, tibiotalar; IT, intertarsal; MTP, metatarsophalangeal.

GS/PD	No	R/L	Finger Palmer FD 1	2	3	4	5	Wrist Dorsal Comp 2	4	6	Palmer ET	Shoulder Anterior LHB	Ankle Extensor EDL	EHL	TA	Medial TP	FDL	Lateral PL	PB	Toe Plantar FD 1	2	3	4	5	Total
GS	1	R	0	1	1	1	1	1	1	1	0	0	1	0	0	0	0	0	0	0	0	0	0	0	17
		L	1	1	1	1	1	1	1	1	0	0	1	0	0	0	0	0	0	0	0	0	0	0	
	2	R	2	2	2	2	1	1	2	1	0	0	2	1	3	0	0	1	1	0	0	0	0	0	38
		L	0	2	2	2	1	1	1	0	0	0	2	2	2	1	0	2	1	0	0	0	0	0	
	3	R	0	0	0	0	0	0	0	0	0	1	1	0	0	0	0	0	0	0	0	0	0	0	4
		L	0	1	1	0	0	0	0	0	0	1	1	0	0	0	0	0	0	0	0	0	0	0	
	4	R	0	2	1	2	3	1	2	1	0	1	3	0	1	1	0	1	1	0	0	0	0	0	38
		L	1	2	2	1	2	0	1	1	0	2	2	3	0	1	0	0	0	0	0	0	0	0	
	5*	R	3	2	3	3	1	2	1	2	1	0	3	2	3	2	2	2	2	3	1	1	0	0	79
		L	3	2	2	2	1	3	2	2	1	1	3	2	3	2	1	3	3	2	1	1	0	0	
	5**	R	0	1	1	1	1	1	0	1	0	0	2	0	2	1	1	1	1	0	0	0	0	0	19
		L	0	0	1	1	0	0	0	0	0	0	1	0	1	0	0	1	0	0	0	0	0	0	
	6*	R	0	1	1	1	1	2	2	1	0	1	2	0	1	1	1	1	1	0	0	0	0	0	44
		L	0	1	2	2	1	1	1	2	0	1	2	0	1	1	0	1	1	0	0	0	0	0	
	6**	R	0	0	0	0	0	1	0	0	0	0	0	0	0	1	0	0	0	0	0	0	0	0	6
		L	0	0	0	0	0	1	0	1	0	0	1	0	0	1	0	0	0	0	0	0	0	0	
	7	R	0	0	0	0	0	3	1	0	0	0	2	1	2	2	2	1	1	0	0	0	0	0	25
		L	0	0	0	0	0	1	2	1	0	0	0	1	0	2	1	1	1	0	0	0	0	0	
	8	R	1	1	2	2	2	2	2	1	0	0	2	0	2	2	2	2	2	0	0	0	0	0	51
		L	1	1	1	1	1	3	2	2	0	1	2	1	3	2	1	2	2	0	0	0	0	0	
	9	R	0	0	0	0	0	0	1	1	0	0	0	0	0	0	0	0	1	0	0	0	0	0	8
		L	0	0	1	0	0	1	0	1	0	0	1	0	0	1	0	0	0	0	0	0	0	0	
	10	R	0	0	0	0	0	1	0	0	0	0	2	0	0	1	1	2	1	0	0	0	0	0	11
		L	0	0	0	0	0	0	0	0	0	0	1	0	0	0	0	1	1	0	0	0	0	0	
PD	1	R	0	0	0	0	0	0	0	0	0	0	0	0	0	0	0	0	0	0	0	0	0	0	0
		L	0	0	0	0	0	0	0	0	0	0	0	0	0	0	0	0	0	0	0	0	0	0	
	2	R	1	2	1	1	0	0	2	2	0	0	1	0	2	0	0	0	0	0	0	0	0	0	12
		L	0	2	1	1	0	0	0	0	0	0	1	2	2	0	0	0	0	0	0	0	0	0	
	3	R	0	0	0	0	0	0	0	0	0	0	0	0	0	0	0	0	0	0	0	0	0	0	0
		L	0	0	0	0	0	0	0	0	0	0	0	0	0	0	0	0	0	0	0	0	0	0	
	4	R	0	0	0	1	0	0	1	0	0	0	0	0	0	0	0	0	0	0	0	0	0	0	4
		L	0	0	0	0	0	0	0	0	0	1	0	1	0	0	0	0	0	0	0	0	0	0	
	5*	R	3	2	3	3	1	2	2	2	1	0	3	1	3	2	2	2	2	2	0	0	0	0	72
		L	3	3	3	2	1	3	1	1	2	0	3	1	3	2	1	2	2	1	2	0	0	0	
	5**	R	0	0	0	0	0	1	0	1	0	0	2	0	0	1	1	0	0	0	0	0	0	0	8
		L	0	0	0	0	0	0	0	0	0	0	0	0	0	0	0	2	0	0	0	0	0	0	
	6*	R	0	2	1	1	0	3	1	2	0	1	2	0	0	0	0	1	1	0	0	0	0	0	24
		L	0	1	0	1	0	1	1	2	0	1	2	0	0	0	0	0	0	0	0	0	0	0	
	6**	R	0	0	0	0	0	0	0	0	0	0	0	0	0	0	0	0	0	0	0	0	0	0	0
		L	0	0	0	0	0	0	0	0	0	0	0	0	0	0	0	0	0	0	0	0	0	0	
	7	R	0	0	0	0	0	3	2	0	0	0	2	1	1	2	2	0	0	0	0	0	0	0	23
		L	0	0	0	0	0	2	3	0	0	0	0	1	0	2	0	1	1	0	0	0	0	0	
	8	R	0	2	2	2	2	2	3	0	0	0	1	0	1	0	0	0	0	0	0	0	0	0	34
		L	0	1	1	1	1	3	2	3	0	0	1	1	1	1	1	1	1	0	0	0	0	0	
	9	R	0	0	0	0	0	0	0	0	0	0	0	0	0	0	0	0	0	0	0	0	0	0	1
		L	0	0	1	0	0	0	0	0	0	0	0	0	0	0	0	0	0	0	0	0	0	0	
	10	R	0	0	0	0	0	0	0	0	0	0	0	0	0	0	0	1	0	0	0	0	0	0	1
		L	0	0	0	0	0	0	0	0	0	0	0	0	0	0	0	0	0	0	0	0	0	0	

☐ Grade 0   ☐ Grade 1   ☐ Grade 2   ☐ Grade 3

Figure 2 Ultrasound scores for tenosynovitis in patients with Blau syndrome. Semiquantitative grades (0 to 3) for gray-scale synovitis and synovial power Doppler signal in individual joint regions are shown with heat maps. Total sum of the scores in each case is shown in the rightmost column. *First ultrasound examination (before treatment); **second ultrasound examination (after treatment). GS, gray-scale; PD, power Doppler; No, case number; R, right; L, left; FT, flexor tendon; Comp, compartment; ETs, extensor tendons (flexor digitorum superficialis/profundus and flexor carpi radialis); LHB, long head of biceps tendon; EDL, extensor digitorum longus; EHL, extensor hallucis longus; TA, tibialis anterior; TP, tibialis posterior; FDL, flexor digitorum longus; PL, peroneus longus; PB, peroneus brevis.

2, moderate; grade 3, severe) based on the rater's impression of how large the volume of synovial hypertrophy and synovial fluid was for the synovial site assessed. On the other hand, synovial PD signal was graded as a PD score on a scale of 0 to 3 (grade 0, normal; grade 1, mild; grade 2, moderate; grade 3, severe) based on the rater's impression of how widespread the abnormal synovial PD signals within the synovial hypertrophy were. Total scores for an individual patient were calculated for each synovial tissue and for all synovial tissues by summation for each synovial tissue (that is, total intra-articular GS/PD score, total tenosynovial GS/PD score, total bursal GS/PD score) and for all synovial tissues (that is, total synovial GS/PD score). When ultrasound findings were assessed at a 40-joint level, the maximum grade obtained from multiple synovial sites (for example, radiocarpal joint, extensor carpi

ulnaris) within a joint unit was assigned to the joint (for example, wrist).

Statistical analysis

Statistical analysis was performed using R version 2.13.0 (The R Foundation for Statistical Computing, Vienna, Austria). Non-normally distributed continuous data were analyzed using nonparametric tests (Spearman's rank correlation coefficient and Wilcoxon signed-rank test). Categorical data were analyzed using McNemar's test. Bonferroni's correction was applied for multiple testing. *P*-values less than 0.05 were considered statistically significant.

Results

Demographics and disease characteristics

Ten patients (two female) from eight unrelated Japanese families enrolled in this study. As shown in Table 1, the age at ultrasound examination ranged from 10 months to 37 years and the patients were numbered from 1 to 10 in order of this age. Patients 1, 2, and 10 were offspring and a parent, whereas the other patients had no family history suggestive of Blau syndrome. All patients had been shown to have a known *NOD2* gene mutation associated with Blau syndrome (Table 1). Patient 3 was an atypical case who developed aortitis at the age of 7 months, which was treated successfully with corticosteroid (pulse methylprednisolone followed by oral prednisolone for 5 years), methotrexate, and infliximab as infantile Takayasu arteritis. He was genotyped for *NOD2* when he developed iritis at the age of 7 years [39].

Treatment at ultrasound examination

Three patients (patients 1, 5, and 10) were not receiving any medication for joint involvement when ultrasound was performed, and seven patients were receiving anti-inflammatory/rheumatic medications, including non-steroidal anti-inflammatory drugs (NSAIDs), corticosteroids (prednisolone ≤11.25 mg/day), methotrexate, and TNF antagonists (Table 1). In patient 5, treatment with methotrexate plus infliximab was initiated after the first ultrasound examination and the second ultrasound examination was performed after 14 weeks of treatment. In patient 6, infliximab was added to his treatment regimen after the first ultrasound examination and the second ultrasound examination was performed after 12 months.

Severity of arthritis assessed by conventional measures

Table 2 summarizes the severity of arthritis at ultrasound examination. Although swollen joint counts varied among patients, most of the patients did not have any tender joints and therefore, the patient's or parent's global VAS score was ≤10 mm in most of the patients. The levels of acute inflammatory responses and physician's global VAS score were not markedly elevated either. As shown in Table 2, disease activity parameters in patient 5 substantially improved after treatment with methotrexate plus infliximab, whereas the decrease in those parameters in patient 6 was relatively mild.

Camptodactyly was present at least in one joint in patients 4 to 10, whose ages were 9 years and 7 months or older (Table 2). Proximal interphalangeal (PIP) joints were the joints in which camptodactyly was identified most frequently. Despite the presence of multiple

Table 1 Demographics, disease characteristics, and treatment at ultrasound examination

Patient number	NOD2 mutation	Age (months)				Duration of treatment at ultrasound examination (months)			
		At ultrasound examination	At onset of joint symptom	At onset of skin lesion	At diagnosis of uveitis	NSAID	Corticosteroid	Methotrexate	TNF antagonist
1[†]	R334W	10	NA	6	NA	NA	NA	NA	NA
2[†] ref [34]	R334W	66	19	6	NA	NA	NA	13	NA
3 ref [36]	D382E	111	NA	NA	88	NA	NA	60	11 (infliximab)
4	R587C	115	53	NA	NA	NA	NA	32	32 (etanercept)
5	R334W	146*	24	7	39	NA	NA	NA	NA
		154**				NA	NA	3	3 (infliximab)
6	R334W	153*	29	21	35	12	112	124	NA
		166**				NA	NA	137	12 (infliximab)
7 ref [6]	R334Q	160	52	NA	NA	105	NA	60	44 (infliximab)
8 ref [6]	R334W	212	24	8	48	188	142	184	NA
9 ref [6]	R334Q	294	34	24	60	270	259	135	45 (infliximab)
10[†] ref [3]	R334W	452	NR[‡]	24	156	NA	NA	NA	NA

ref: Reference number in which the patient was previously reported; [†]offspring and parent; *1st ultrasound examination; **2nd ultrasound examination; [‡]reported no arthritic symptoms despite the presence of overt camptodactyly. NSAID, non-steroidal anti-inflammatory drug; TNF, tumor necrosis factor; NR, not reported; NA, not applicable.

Table 2 Conventional activity measures for joint inflammation, physical function, and the presence of camptodactyly

Patient number	Tender joint count		Swollen joint count		Global assessment VAS (/100 mm)		Acute inflammatory response (normal range[§])		DAS28 -ESR	DAS28 -CRP	MMP-3[§§] (ng/mL)	CHAQ	Campto- dactyly
	/28	/40	/28	/40	Patient/parent	Physician	ESR, mm/h	CRP, mg/L					
1	NR[†]	NR[†]	0	0	0	2	3 (2 to 10)	3.0 (0 to 3)	NA	NA	27.2	0	No
2	0	0	22	24	10	5	6 (2 to 10)	1.0 (0 to 3)	2.7	2.7	85.3	0	No
3	0	0	0	0	0	3	29 (2 to 10)	32.0 (0 to 3)	2.4	2.2	24.9	0	No
4	0	0	1	1	8	6	19 (3 to 15)	0.7 (0 to 2.6)	2.5	1.5	64.0	0.13	Yes
5*	0	0	23	25	10	50	22 (1 to 10)	6.0 (0 to 3)	3.7	3.1	800.0	0	Yes
5**	0	0	7	9	0	23	3 (1 to 10)	0.0 (0 to 3)	1.5	1.7	21.8	0	Yes
6*	0	0	2	3	1	5	3 (5 to 13)	3.0 (0 to 2)	1.3	1.9	18.7	0	Yes
6**	0	0	2	2	2	1	2 (5 to 13)	0.4 (0 to 2)	0.9	1.5	18.8	0	Yes
7	0	0	1	1	0	0	27 (3 to 15)	1.4 (0 to 2.6)	2.6	1.6	426.4	0	Yes
8	4	4	13	13	65	45	8 (2 to 10)	1.0 (0 to 2.6)	4.5	4.3	36.9	0.63	Yes
9	0	0	0	0	15	8	4 (2 to 10)	0.0 (0 to 2.6)	1.2	1.2	216.8	1.63[‡]	Yes
10	0	0	3	5	4	8	12 (2 to 10)	1.0 (0 to 3)	2.3	1.8	129.0	0.13[‡]	Yes

*1st ultrasound examination ; **2nd ultrasound examination; [†]not reported because the patient was not able to understand and answer the question; [‡]health assessment questionnaire-damage index (HAQ-DI) for adult was obtained; [§]normal range in the institute for patient's sex is provided; [§§]normal ranges are 36.9 to 121.0 ng/mL for males and 17.3 to 59.7 ng/mL for females. VAS, visual analogue scale; ESR, erythrocyte sedimentation rate; CRP, C-reactive protein; DAS28, disease activity score 28; MMP-3, matrix metalloproteinase-3; CHAQ, childhood-health assessment questionnaire; NR, not reported; NA, not applicable.

swollen joints and camptodactyly, physical function assessed by CHAQ/HAQ was rarely impaired in patients younger than 13 years. Photographs of the hands and the right foot and radiographs of the hands in patient 5 are shown in Figures 3 and 4, respectively.

Distribution of inflammation in synovial tissues determined by ultrasound

All patients completed the comprehensive ultrasound assessment of 102 synovial sites. The distribution and the grade of GS and PD scores in each patient were illustrated
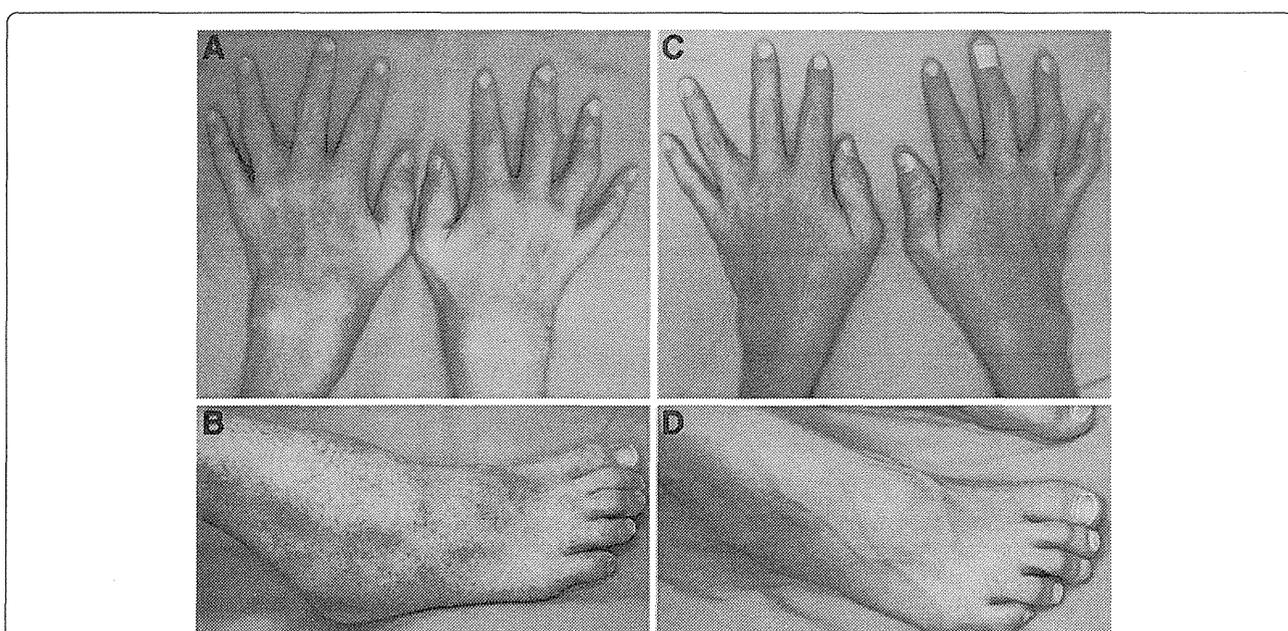
Figure 3 Photographs of the hands and the right foot in patient 5. Shown are the photographs of the hands **(A, C)** and the right foot **(B, D)** in Patient 5 before treatment **(A, B)** and after treatment **(C, D)**. Soft tissue swelling in the wrists, the fingers, the ankle, and the mid foot improved after treatment with methotrexate and infliximab. Papular rash also markedly improved.
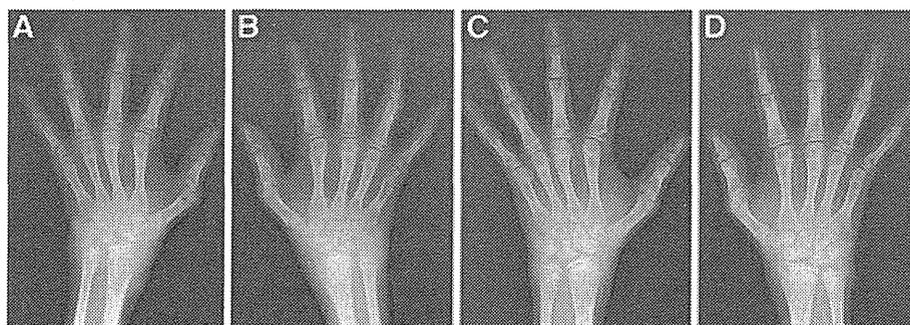
Figure 4 Radiographs of the hands in patient 5. Shown are the radiographs of the left hand **(A, C)** and the right hand **(B, D)** in patient 5 before treatment **(A, B)** and after treatment **(C, D)**. Soft tissue swelling in the wrist and fingers improved after treatment with methotrexate and infliximab.

in heat maps for intra-articular synovitis (Figure 1) and for tenosynovitis (Figure 2). Bursitis was identified only in the sub-acromial/deltoid bursa in bilateral shoulders in one patient (patient 6) with a GS score of 2 bilaterally and a PD score of 2 in the right shoulder (data not shown).

As demonstrated in Figures 1 and 2, a wide range of synovial sites were affected, mostly in a symmetrical manner. Representative ultrasound images of patient 5

are shown in Figure 5. Additional movie files show these in more detail (see Additional files 1, 2, 3, 4, 5 and 6). The most frequently and severely involved synovial sites were tendon sheaths in the ankle, extensor tendon sheaths in the wrist, and the PIP joints. In contrast, some synovial sites, such as the glenohumeral joint, the midtarsal joint, and the olecranon bursa, did not exhibit synovial inflammation on ultrasound.
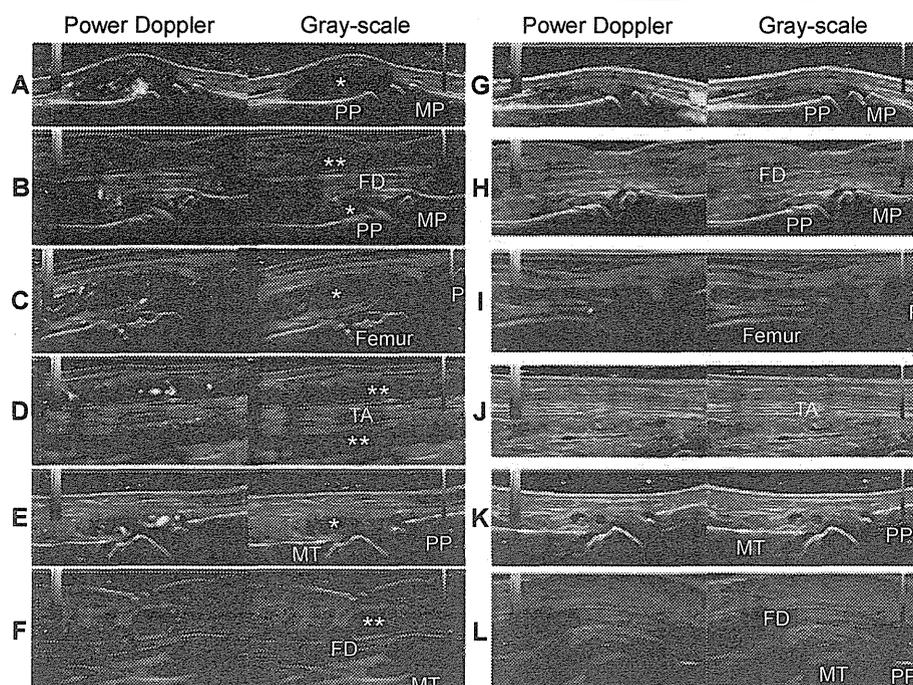
Figure 5 Representative ultrasound images of intra-articular synovitis and tenosynovitis in patient 5. Shown are the representative ultrasound images of intra-articular synovitis **(A, C, E, G, I, K)** and tenosynovitis **(B, D, F, H, J, L)** in patient 5 before **(A-F)** and after treatment **(G-L)**. All images before treatment demonstrate synovial/tenosynovial hypertrophy, which accompanies increased power Doppler signals **(A-F)**. Additional movie files show this in more detail (see Additional files 1, 2, 3, 4, 5 and 6). **(A and G)** Longitudinal view of the dorsal aspect of the 3rd proximal interphalangeal joint in the right hand; **(B and H)** longitudinal view of the flexor tendon of the third finger on the right hand; **(C and I)** oblique view of the anterior-lateral aspect of the suprapatellar recess in the right knee; **(D and J)** a longitudinal view of the tibialis anterior tendon in the right ankle; **(E and K)** longitudinal view of the dorsal aspect of the third metatarsophalangeal joint of the right foot; **(F and L)** longitudinal view of the flexor tendon of the first toe of the right foot. *Intra-articular synovial hypertrophy; **tenosynovial hypertrophy. PP, proximal phalanx; MP, metacarpal; FD, flexor digitorum; TA, tibialis anterior; MT, metatarsal.

Ten age- and sex-matched control subjects, two female, mean age 169.8 months old (range 3 to 499) also underwent comprehensive ultrasound assessment. Only mild GS intra-articular synovitis and tenosynovitis without a PD signal was identified in subjects aged 3 years or older. GS intra-articular synovitis was identified in nine sites in eight joints (three wrists, three toes) in four patients and GS tenosynovitis was identified in five sites in four joints (three ankles) in four patients. These data indicate that GS scores of 2 or greater and positive PD scores have pathological meanings, whereas GS scores of 1 are less specific in our study.

Predominance of tenosynovitis over intra-articular synovitis

Tenosynovitis was more prevalent and more severe than intra-articular synovitis in our patients with Blau syndrome (Figures 1 and 2). When compared in the total joints where both intra-articular- and teno-synovitis were evaluated (that is, elbow and knee joints were excluded), the proportion of the joints with a positive GS score for tenosynovitis was significantly higher than that for intra-articular synovitis (41.5% versus 27.9%, P <0.0001, McNemar test with Bonferroni correction). When compared in each joint, the prevalence of GS tenosynovitis was significantly higher than that of GS intra-articular synovitis in the metacarpophalangeal (MCP) joints (56.0% versus 25.0%, P <0.0001), in the wrist (80.0% versus 30.0%, P = 0.0266), and in the ankle (100% versus 20.0%, P = 0.0011) (McNemar test with Bonferroni correction) (Figure 6A). Similarly, the proportion of the joints with a positive PD score for tenosynovitis was significantly higher than that for intra-articular synovitis in the total joints (22.2% versus 15.2%, P <0.0001), and individually, in the wrist (55.0% versus 15.0%, P = 0.0460) and in the ankle (60.0% versus 0.0%, P = 0.0090) (McNemar test with Bonferroni correction) (Figure 6B). In addition, the GS and PD scores for tenosynovitis were significantly higher than those for intra-articular synovitis in the total joints (P <0.0001 for both scores, Wilcoxon signed-rank test with Bonferroni correction).

Improvement of ultrasound findings after initiating the treatment with infliximab

In patient 5, clinical, radiographic, and ultrasonographic findings markedly improved after 14 weeks of treatment with methotrexate plus infliximab (total intra-articular GS score, 89 versus 13; total intra-articular PD score, 80 versus 7; total tenosynovial GS score, 79 versus 19; total tenosynovial PD score, 72 versus 8) (Figures 1, 2, 3, 4 and 5). This result suggests that treatment with methotrexate plus infliximab can improve the inflammation in synovial tissues in a patient with Blau syndrome in a relatively short period of time.

Adding infliximab to methotrexate also substantially improved the ultrasound findings in patient 6, leaving no residual PD signals in the synovial tissues even after the corticosteroid and the NSAID were discontinued (total intra-articular GS score, 20 versus 10; total intra-articular PD score, 7 versus 0; total tenosynovial GS score, 44 versus 6; total tenosynovial PD score, 24 versus 0) (Figures 1 and 2). These data indicate that ultrasound scores are more responsive to change as compared with conventional measures.

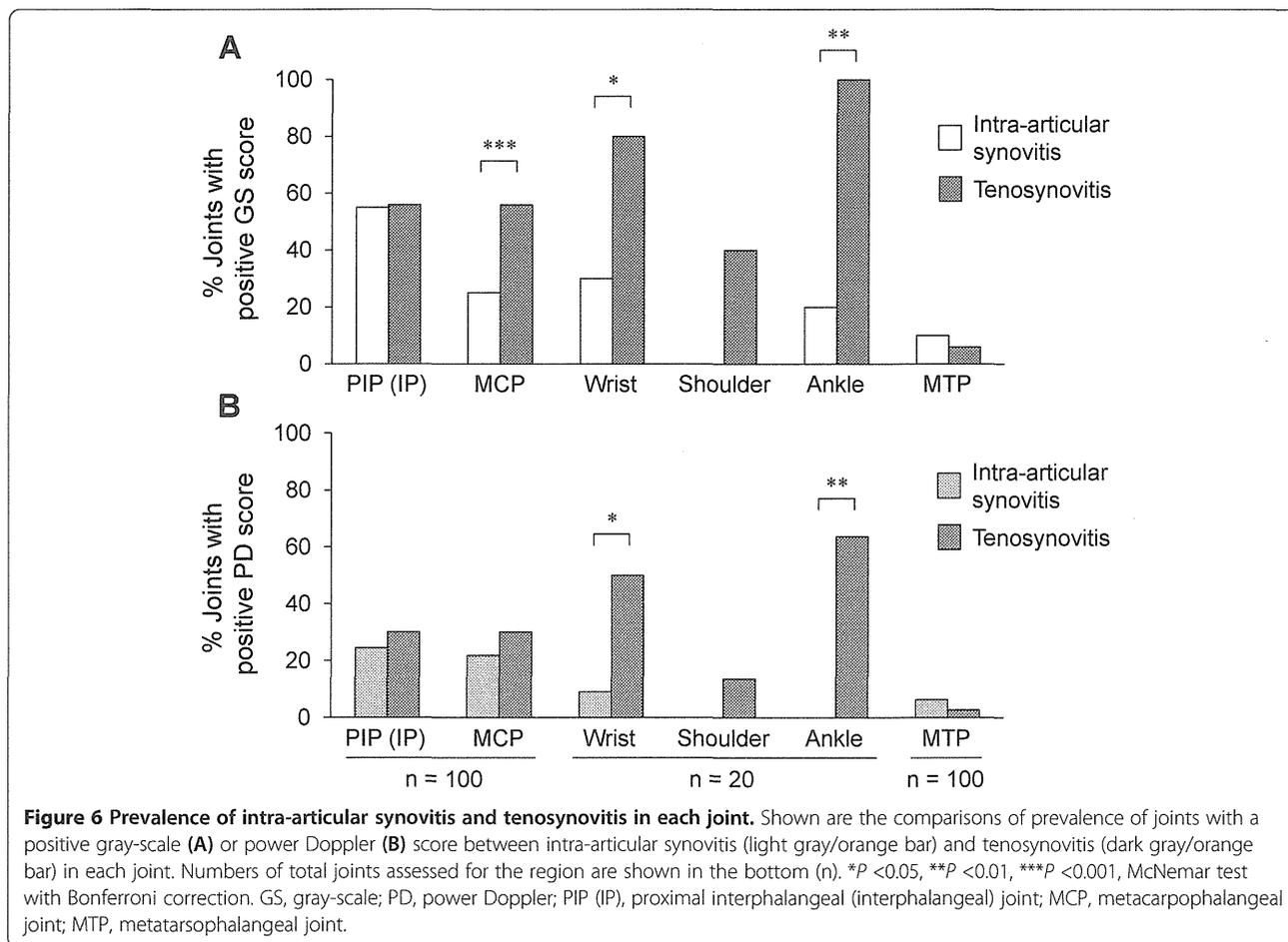## Influence of age and treatment on inflammation in synovial tissues

Also demonstrated in Figures 1 and 2, together with Table 1, is the influence of age and treatment on synovial inflammation. Focusing on the PD score, severe cases of intra-articular synovitis clustered between patient 5 (12 years and 2 months old) and patient 8 (18 years and 8 months old) (Figure 1). On the other hand, severe cases of tenosynovitis clustered between patient 2 (5 years and 6 months old) and patient 8 (Figure 2). Of note, ultrasound revealed little or no inflammation accompanying the PD signal in patient 1 (10 months old) and patient 10 (37 years and 8 months old) even though they had never received anti-inflammatory or rheumatic treatment, whereas patient 2, who is a member of the same family carrying the same *NOD2* mutation, exhibited substantial PD tenosynovitis despite receiving an NSAID and methotrexate. Patients within the cluster whose ultrasound images showed relatively mild PD signals (patients 3, 4, 5 (after treatment) and 6 (after treatment)) were all receiving treatment with methotrexate plus a TNF antagonist.

Discrepancy between ultrasound scores and conventional measures for the activity of arthritis

As shown in Table 3, the swollen joint count tended to correlate with total ultrasound scores (ρ 0.68 to 0.76, P 0.0364 to 0.1343). However, no other conventional measures for arthritis activity correlated with total ultrasound scores with statistical significance.

At a 40-joint level, numbers of joints with tenderness, swelling, GS $\geq$1 synovitis (GS score $\geq$1), GS $\geq$2 synovitis (GS score $\geq$2), and synovial PD signal were 4 (0.8%), 81 (16.9%), 240 (50.0%), 117 (24.4%), and 124 (25.8%), respectively. The differences in prevalence between swelling and ultrasound findings were statistically significant (swelling versus GS $\geq$1 synovitis, P <0.0001; swelling versus GS $\geq$2 synovitis, P = 0.0002; swelling versus synovial PD signal, P <0.0001) (McNemar test with Bonferroni correction). Importantly, GS $\geq$1/GS $\geq$2 synovitis was present in 168/57 out of 399 non-swollen joints, in which 61 also exhibited synovial PD signal (Table 4).

In each joint region, prevalence of GS $\geq$1 synovitis was significantly higher than that of joint swelling in the

Figure 6 Prevalence of intra-articular synovitis and tenosynovitis in each joint. Shown are the comparisons of prevalence of joints with a positive gray-scale **(A)** or power Doppler **(B)** score between intra-articular synovitis (light gray/orange bar) and tenosynovitis (dark gray/orange bar) in each joint. Numbers of total joints assessed for the region are shown in the bottom (n). *P <0.05, **P <0.01, ***P <0.001, McNemar test with Bonferroni correction. GS, gray-scale; PD, power Doppler; PIP (IP), proximal interphalangeal (interphalangeal) joint; MCP, metacarpophalangeal joint; MTP, metatarsophalangeal joint.

PIP joints (73.3% versus 24.2%, P <0.0001), the MCP joints (55.0% versus 15.0%, P <0.0001), and the ankle (100% versus 37.6%, P = 0.0072) (McNemar test with Bonferroni correction) (Figure 7). Prevalence of GS ≥1 synovitis and synovial PD signal were also significantly higher than that of joint swelling in the MCP joints (29.2% and 31.7% versus 15.0%, P = 0.0058 and P = 0.0012, respectively, McNemar test with Bonferroni correction) (Figure 7).

Discussion

In this multi-center study, ultrasonographic assessment of 102 synovial sites provided detailed information on the anatomical distribution of synovial inflammation in patients with Blau syndrome. Our data demonstrate that a wide range of synovial sites can be affected mostly in a symmetrical manner in patients with Blau syndrome. Most frequently involved joints identified in this study are

Table 3 Correlation between total ultrasound scores and conventional activity measures

		Tender joint count /40	Swollen joint count /40	Patient's VAS	Physician's VAS	ESR	CRP	DAS28 -ESR	DAS28 -CRP	MMP-3
Intra-articular synovium	**Total GS score**	0.30	0.76*	0.36	0.51	0.21	0.11	0.53	0.55	0.19
	Total PD score	0.35	0.69	0.18	0.40	0.20	0.25	0.63	0.61	0.45
Tenosynovium	**Total GS score**	0.00	0.68	0.42	0.47	0.13	0.21	0.67	0.57	0.45
	Total PD score	0.55	0.72	0.40	0.51	0.23	0.17	0.66	0.59	0.30
Total	**Total GS score**	0.20	0.72	0.34	0.39	0.21	0.28	0.67	0.59	0.33
	Total PD score	0.37	0.68	0.35	0.51	0.27	0.12	0.66	0.53	0.25

Values are Spearman's correlation coefficients (ρ). *P < 0.05; no other correlations were statistically significant when Bonferroni correction was applied. VAS, visual analogue scale; ESR, erythrocyte sedimentation rate; CRP, C-reactive protein; DAS28, disease activity score 28; MMP-3, matrix metalloproteinase-3; GS, gray-scale; PD, power Doppler.

Table 4 Discrepancy between joint swelling and ultrasound findings

		Swelling		Total
		(−)	(+)	
Gray-scale synovitis	(−)	231 (48)	9 (2)	240 (50)
(gray-scale score ≥1)	(+)	168 (35)	72 (15)	240 (50)
Total		399 (83)	81 (17)	480 (100)
Gray-scale synovitis	(−)	342 (71)	21 (4)	363 (75)
(gray-scale score ≥2)	(+)	57 (12)	60 (13)	240 (25)
Total		399 (83)	81 (17)	480 (100)
Synovial	(−)	338 (70)	18 (4)	356 (74)
Power Doppler signal	(+)	61 (13)	63 (13)	124 (26)
Total		399 (83)	81 (17)	480 (100)

Values are the number (%) of joint regions.

consistent with the previous reports [1,7,13-15]. However, our data provide novel and more specific information on the anatomical site (intra-articular synovium versus tenosynovium versus bursa), the chronicity (currently active inflammation versus chronic swelling versus subsequent contracture), and the severity (mild versus severe). As a result, the data in the form of a heat map (Figures 1 and 2) readily provide clinicians and researchers with valuable information. Furthermore, our data for the first time demonstrate the predominance of tenosynovitis over intra-articular synovitis in Blau syndrome. Although frequent involvement of the tenosynovium has been reported descriptively [1,7,13-15], no studies had provided objective data on the predominance of tenosynovitis.
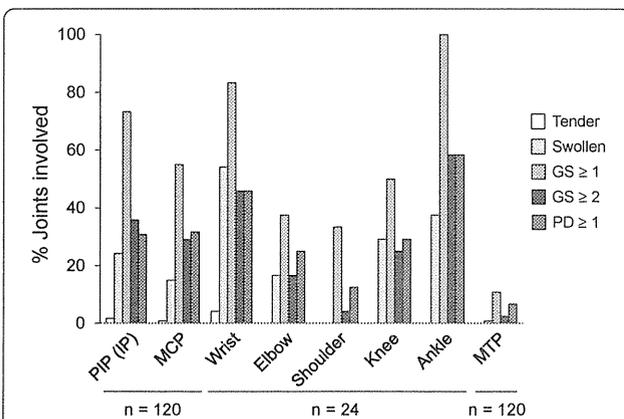
Figure 7 Prevalence of clinical manifestations and ultrasound findings in each joint. Shown are the proportions of joints with tenderness (white bar), swelling (light blue bar), gray-scale synovitis ≥ grade 1 (light gray bar), gray-scale synovitis ≥ grade 2 (dark gray bar), and synovial power Doppler signal (orange bar). Numbers of total joints assessed for the region are shown in the bottom (n). **P <0.01, ***P <0.001, McNemar test with Bonferroni correction. GS, gray-scale score; PD, power Doppler score; PIP (IP), proximal interphalangeal (interphalangeal) joint; MCP, metacarpophalangeal joint; MTP, metatarsophalangeal joint.

Although this is a cross-sectional study except for patient 5 and 6, comprehensive and detailed data from patients at a wide range of ages who share the same underlying molecular pathophysiology let us speculate on the natural history of synovial inflammation in Blau syndrome. Comparing the siblings (patients 1 and 2), we assume that mild GS tenosynovitis precedes clinically detectable joint swelling and full-blown PD-positive tenosynovitis; we also assume that tenosynovitis precedes intra-articular synovitis. Given the minimal PD activity of synovial inflammation in patient 10, who carries the same *NOD2* mutation as patient 2 but has never received treatment, we also speculate that active synovial inflammation can spontaneously ameliorate, at least in some patients with Blau syndrome, at some point after their adolescence. These hypotheses, however, need to be confirmed in a large-scale observational study.

The marked improvement in PD scores in patients 5 and 6 after treatment with methotrexate plus infliximab and relatively low total PD scores in patients receiving treatment with methotrexate plus TNF antagonists (patients 3, 4, 7, and 9) support the notion that a methotrexate plus TNF antagonist regimen is efficacious not only for RA [40,41] and JIA [42] but also for arthritis in patients with Blau syndrome [43]. On the other hand, the effectiveness of methotrexate monotherapy was not obvious in our small group of patients. We do not exclude the possible influence of genotypes on the severity of arthritis in patient 3 (D382E) and 4 (R587C), both of which were not included in the previous analysis of the association between genotype and phenotype [6]. A future investigation on the association between *NOD2* genotypes and ultrasound-defined severity of arthritis in a larger number of patients may identify the high-risk genotypes for severe synovial inflammation.

The symmetrical involvement of synovial tissues and the effectiveness of methotrexate plus infliximab in our patients with Blau syndrome support the argument that autoinflammatory diseases such as Blau syndrome and autoimmune diseases such as RA share some phenotypic manifestations and cytokine pathways that maintain arthritis even though the contribution of innate/acquired immunity to pathogenesis is quite different between these two categories of disease [44]. However, our study also confirms the painless nature of arthritis in Blau syndrome, which contrasts with RA. Our patients exhibited surprisingly little tenderness or pain (Table 2) in the presence of active inflammation in both the intra-articular- and tenosynovium (Figures 1 and 2). In addition, the elevation of acute inflammatory responses was infrequent and mild, which is consistent with some of the previous reports [1,14]. These data were reflected in the poor correlations of total ultrasound scores with tender joint count, patients'/parents' global VAS, ESR, and CRP (Table 3),

indicating that these measures do not reflect synovial inflammation in Blau syndrome. The reasons for this absence of canonical features of inflammation in the presence of synovial inflammation, along with the predominance of tenosynovitis, caused by *NOD2* mutations are intriguing research questions in understanding the molecular mechanisms of inflammation.

On the other hand, the swollen joint count tended to correlate with total ultrasound scores (Table 3), suggesting that the swollen joint count is the most reliable conventional measure that can reflect the global severity of synovial inflammation in patients with Blau syndrome. At a joint level, however, active synovial inflammation was frequently detected by ultrasound in joints without swelling (Table 4). These data indicate that clinically detected joint swelling is not as sensitive as ultrasound findings to represent synovial inflammation.

Given the significant improvement of clinical parameters after treatment in patient 5 (Table 2), these measures may reflect the therapeutic effect of potent therapy on arthritis when disease activity is very high. However, in order to prevent structural damage and late-onset functional impairment, treating patients to a minimal disease activity state, which can be only evaluated by ultrasound, may be important. Since the impact of synovial inflammation on structural and functional deterioration in Blau syndrome can be substantially different from that in RA and JIA, longitudinal assessment of arthritis in Blau syndrome using quantitative measures for structural damage (for example, radiographic score) is urgently needed to determine the threshold of acceptable activity of synovial inflammation. In the future, clinical studies to establish optimized treatment strategies (for example, treatment agent, treatment target) for arthritis in Blau syndrome, ultrasound may play a significant role in decreasing the sample size needed by providing better quantification and sensitivity to change.

One of the major limitations of our study is the very small sample size. However, Blau syndrome is a much more homogeneous condition as compared with RA or JIA, especially when the genetic mutation of *NOD2* is confirmed. Also given the quantitative capability and the excellent reproducibility of ultrasonographic assessment of synovial inflammation in the recent reports [22,29,36,37], the comprehensive data obtained in this study are likely to represent the pathophysiology of arthritis in Blau syndrome and provide more reliable information than the mostly descriptive one in the previous reports.

Another major limitation of our study is that ultrasonographic synovial pathologies were graded subjectively due to the lack of currently available standardized measures for children. Although our data support the use of ultrasound in monitoring the disease activity of Blau syndrome, our data cannot be readily generalizable and need to be

confirmed in future studies when standardized methods are established. Furthermore, performing the comprehensive ultrasound assessment we employed in this study is not feasible in daily practice. The essential synovial sites to be scanned should be determined not only by the frequency of involvement, but also by the impact on structural and functional deterioration in Blau syndrome. Although we assume that PD signal is more essential than GS synovitis in monitoring disease activity, careful gray-scale assessment is fundamentally important to distinguish between the inflammatory angiogenesis in synovial hypertrophy and the feeding vessels in unossified cartilage in children.

Conclusions

The detailed anatomical distribution and severity of synovial inflammation revealed by comprehensive ultrasound assessment confirm the frequently involved joints, the predominance of tenosynovitis, and the dissociation between pain and inflammation in the arthritis of Blau syndrome. Our data also give an insight into the treatment response of arthritis in Blau syndrome and demonstrate that musculoskeletal ultrasound can be a potent tool in monitoring the activity of synovial inflammation and in investigating the pathophysiology of arthritis in this rare but archetypical autoinflammatory condition.

Additional files

Additional file 1: A longitudinal view of the dorsal aspect of the 3rd proximal interphalangeal joint in the right hand. Severe synovial hypertrophy accompanies severe power Doppler signals.

Additional file 2: A longitudinal view of the flexor tendon of the 3rd finger in the right hand. Moderate tenosynovial hypertrophy accompanies moderate power Doppler signals. Transverse views of this lesion showed more severe findings.

Additional file 3: An oblique view of the anterior-lateral aspect of the suprapatellar recess in the right knee. Severe synovial hypertrophy accompanies severe power Doppler signals.

Additional file 4: A longitudinal view of the tibialis anterior tendon in the right ankle. Severe tenosynovial hypertrophy accompanies moderate to severe power Doppler signals.

Additional file 5: A longitudinal view of the dorsal aspect of the 3rd metatarsophalangeal joint in the right foot. Mild to moderate synovial hypertrophy accompanies moderate to severe power Doppler signals.

Additional file 6: A longitudinal view of the flexor tendon of the 1st toe in the right foot. Severe tenosynovial hypertrophy accompanies moderate power Doppler signals.

Abbreviations

CHAQ-DI: childhood health assessment questionnaire-disability index; CRP: C-reactive protein; DAS28: disease activity score 28; EOS: early onset sarcoidosis; ESR: erythrocyte sedimentation rate; GS: gray-scale; HAQ-DIL: health assessment questionnaire-disability index; JIA: juvenile idiopathic arthritis; MCP: metacarpophalangeal; MMP-3: metalloproteinase-3; MTP: metatarsophalangeal; NFκB: nuclear factor kappa-light-chain-enhancer of activated B cells; NOD: nucleotide-binding oligomerization domain; NSAID: nonsteroidal anti-inflammatory drug; PD: power Doppler; PIP: proximal interphalangeal; RA: rheumatoid arthritis; RF: rheumatoid factor; TNF: tumor necrosis factor; VAS: visual analogue scale.

Author details

[1]Department of Allergy and Clinical Immunology, Chiba University Hospital, 1-8-1 Inohana, Chuo-ku, Chiba 260-8677, Japan. [2]Department of Dermatology, Chiba University Graduate School of Medicine, 1-8-1 Inohana, Chuo-ku, Chiba 260-8670, Japan. [3]Division of Pediatric Rheumatology, Pediatric Medical Center, Kagoshima University Hospital, 8-35-1 Sakuragaoka, Kagoshima, Kagoshima 890-8520, Japan. [4]School of Health Sciences, Faculty of Medicine, Kagoshima University, 8-35-1 Sakuragaoka, Kagoshima, Kagoshima 890-8520, Japan. [5]Department of Pediatrics, Chiba University Graduate School of Medicine, 1-8-1 Inohana, Chuo-ku, Chiba 260-8670, Japan. [6]Department of Allergy and Rheumatology, Chiba Children's Hospital, 579-1 Hetacho, Midori-ku, Chiba 266-0007, Japan. [7]Department of Pediatrics, Hitachinaka General Hospital, 20-1 Ishikawacho, Hitachinaka, Ibaraki 312-0057, Japan. [8]Department of Pediatrics, Kobe City Medical Center General Hospital, 2-1-1 Minatojima-minamimachi, Chuo-ku, Kobe, Hyogo 650-0047, Japan. [9]Department of Dermatology, Wakayama Medical University, 811-1 Kimiidera, Wakayama, Wakayama 641-0012, Japan. [10]Department of Pediatrics, Kyoto University Graduate School of Medicine, Yoshida-Konoe-cho, Sakyo-ku, Kyoto 606-8501, Japan.

References

1. Blau EB: Familial granulomatous arthritis, iritis, and rash. *J Pediatr* 1985, 107:689–693.
2. Miceli-Richard C, Lesage S, Rybojad M, Prieur AM, Manouvrier-Hanu S, Hafner R, Chamaillard M, Zouali H, Thomas G, Hugot JP: CARD15 mutations in Blau syndrome. *Nat Genet* 2001, 29:19–20.
3. Kanazawa N, Okafuji I, Kambe N, Nishikomori R, Nakata-Hizume M, Nagai S, Fuji A, Yuasa T, Manki A, Sakurai Y, Nakajima M, Kobayashi H, Fujiwara I, Tsutsumi H, Utani A, Nishigori C, Heike T, Nakahata T, Miyachi Y: Early-onset sarcoidosis and CARD15 mutations with constitutive nuclear factor-kappaB activation: common genetic etiology with Blau syndrome. *Blood* 2005, 105:1195–1197.
4. Rose CD, Doyle TM, McIlvain-Simpson G, Coffman JE, Rosenbaum JT, Davey MP, Martin TM: Blau syndrome mutation of CARD15/NOD2 in sporadic early onset granulomatous arthritis. *J Rheumatol* 2005, 32:373–375.
5. Rose CD, Wouters CH, Meiorin S, Doyle TM, Davey MP, Rosenbaum JT, Martin TM: Pediatric granulomatous arthritis: an international registry. *Arthritis Rheum* 2006, 54:3337–3344.
6. Okafuji I, Nishikomori R, Kanazawa N, Kambe N, Fujisawa A, Yamazaki S, Saito M, Yoshioka T, Kawai T, Sakai H, Tanizaki H, Heike T, Miyachi Y, Nakahata T: Role of the NOD2 genotype in the clinical phenotype of Blau syndrome and early-onset sarcoidosis. *Arthritis Rheum* 2009, 60:242–250.
7. Arostegui JI, Arnal C, Merino R, Modesto C, Antonia Carballo M, Moreno P, Garcia-Consuegra J, Naranjo A, Ramos E, de Paz P, Rius J, Plaza S, Yague J: NOD2 gene-associated pediatric granulomatous arthritis: clinical diversity, novel and recurrent mutations, and evidence of clinical improvement with interleukin-1 blockade in a Spanish cohort. *Arthritis Rheum* 2007, 56:3805–3813.
8. Mathews RJ, Sprakes MB, McDermott MF: NOD-like receptors and inflammation. *Arthritis Res Ther* 2008, 10:228.
9. Lachmann HJ, Hawkins PN: Developments in the scientific and clinical understanding of autoinflammatory disorders. *Arthritis Res Ther* 2009, 11:212.
10. Rose CD, Arostegui JI, Martin TM, Espada G, Scalzi L, Yague J, Rosenbaum JT, Modesto C, Cristina Arnal M, Merino R, Garcia-Consuegra J, Carballo Silva MA, Wouters CH: NOD2-associated pediatric granulomatous arthritis, an expanding phenotype: study of an international registry and a national cohort in Spain. *Arthritis Rheum* 2009, 60:1797–1803.
11. Sfriso P, Caso F, Tognon S, Galozzi P, Gava A, Punzi L: Blau syndrome, clinical and genetic aspects. *Autoimmun Rev* 2012, 12:44–51.
12. Punzi L, Gava A, Galozzi P, Sfriso P: Miscellaneous non-inflammatory musculoskeletal conditions, Blau syndrome. *Best Pract Res Clin Rheumatol* 2011, 25:703–714.
13. North AF Jr, Fink CW, Gibson WM, Levinson JE, Schuchter SL, Howard WK, Johnson NH, Harris C: Sarcoid arthritis in children. *Am J Med* 1970, 48:449–455.
14. Raphael SA, Blau EB, Zhang WH, Hsu SH: Analysis of a large kindred with Blau syndrome for HLA, autoimmunity, and sarcoidosis. *Am J Dis Child* 1993, 147:842–848.
15. Manouvrier-Hanu S, Puech B, Piette F, Boute-Benejean O, Desbonnet A, Duquesnoy B, Farriaux JP: Blau syndrome of granulomatous arthritis, iritis, and skin rash: a new family and review of the literature. *Am J Med Genet* 1998, 76:217–221.
16. Wakefield RJ, Green MJ, Marzo-Ortega H, Conaghan PG, Gibbon WW, McGonagle D, Proudman S, Emery P: Should oligoarthritis be reclassified? Ultrasound reveals a high prevalence of subclinical disease. *Ann Rheum Dis* 2004, 63:382–385.
17. Naredo E, Bonilla G, Gamero F, Uson J, Carmona L, Laffon A: Assessment of inflammatory activity in rheumatoid arthritis: a comparative study of clinical evaluation with grey scale and power Doppler ultrasonography. *Ann Rheum Dis* 2005, 64:375–381.
18. Szkudlarek M, Klarlund M, Narvestad E, Court-Payen M, Strandberg C, Jensen KE, Thomsen HS, Ostergaard M: Ultrasonography of the metacarpophalangeal and proximal interphalangeal joints in rheumatoid arthritis: a comparison with magnetic resonance imaging, conventional radiography and clinical examination. *Arthritis Res Ther* 2006, 8:R52.
19. Brown AK, Conaghan PG, Karim Z, Quinn MA, Ikeda K, Peterfy CG, Hensor E, Wakefield RJ, O'Connor PJ, Emery P: An explanation for the apparent dissociation between clinical remission and continued structural deterioration in rheumatoid arthritis. *Arthritis Rheum* 2008, 58:2958–2967.
20. Freeston JE, Wakefield RJ, Conaghan PG, Hensor EM, Stewart SP, Emery P: A diagnostic algorithm for persistence of very early inflammatory arthritis: the utility of power Doppler ultrasound when added to conventional assessment tools. *Ann Rheum Dis* 2010, 69:417–419.
21. Filer A, de Pablo P, Allen G, Nightingale P, Jordan A, Jobanputra P, Bowman S, Buckley CD, Raza K: Utility of ultrasound joint counts in the prediction of rheumatoid arthritis in patients with very early synovitis. *Ann Rheum Dis* 2011, 70:500–507.
22. Nakagomi D, Ikeda K, Okubo A, Iwamoto T, Sanayama Y, Takahashi K, Yamagata M, Takatori H, Suzuki K, Takabayashi K, Nakajima H: Ultrasound can improve the accuracy of the 2010 american college of rheumatology/european league against rheumatism classification criteria for rheumatoid arthritis to predict the requirement for methotrexate treatment. *Arthritis Rheum* 2013, 65:890–898.
23. Colebatch AN, Edwards CJ, Ostergaard M, van der Heijde D, Balint PV, D'Agostino MA, Forslind K, Grassi W, Haavardsholm EA, Haugeberg G, Jurik AG, Landewe RB, Naredo E, O'Connor PJ, Ostendorf B, Potocki K, Schmidt WA, Smolen JS, Sokolovic S, Watt I, Conaghan PG: EULAR recommendations for the use of imaging of the joints in the clinical management of rheumatoid arthritis. *Ann Rheum Dis* 2013, 72:804–814.
24. Ten Cate DF, Luime JJ, Swen N, Gerards AH, De Jager MH, Basoski NM, Hazes JM, Haagsma CJ, Jacobs JW: Role of ultrasonography in diagnosing early rheumatoid arthritis and remission of rheumatoid arthritis - a systematic review of the literature. *Arthritis Res Ther* 2013, 15:R4.

25. Naredo E, Collado P, Cruz A, Palop MJ, Cabero F, Richi P, Carmona L, Crespo M: Longitudinal power Doppler ultrasonographic assessment of joint inflammatory activity in early rheumatoid arthritis: predictive value in disease activity and radiologic progression. *Arthritis Rheum* 2007, 57:116–124.

26. Naredo E, Moller I, Cruz A, Carmona L, Garrido J: Power Doppler ultrasonographic monitoring of response to anti-tumor necrosis factor therapy in patients with rheumatoid arthritis. *Arthritis Rheum* 2008, 58:2248–2256.

27. Hammer HB, Kvien TK: Comparisons of 7- to 78-joint ultrasonography scores: all different joint combinations show equal response to adalimumab treatment in patients with rheumatoid arthritis. *Arthritis Res Ther* 2011, 13:R78.

28. Wakefield RJ, D'Agostino MA, Naredo E, Buch MH, Iagnocco A, Terslev L, Ostergaard M, Backhaus M, Grassi W, Dougados M, Burmester GR, Saleem B, de Miguel E, Estrach C, Ikeda K, Gutierrez M, Thompson R, Balint P, Emery P: After treat-to-target: can a targeted ultrasound initiative improve RA outcomes? *Ann Rheum Dis* 2012, 71:799–803.

29. Ikeda K, Nakagomi D, Sanayama Y, Yamagata M, Okubo A, Iwamoto T, Kawashima H, Takahashi K, Nakajima H: Correlation of radiographic progression with the cumulative activity of synovitis estimated by power Doppler ultrasound in rheumatoid arthritis: difference between patients treated with methotrexate and those treated with biological agents. *J Rheumatol* 2013, 40:1967–1976.

30. Magni-Manzoni S, Epis O, Ravelli A, Klersy C, Veisconti C, Lanni S, Muratore V, Scire CA, Rossi S, Montecucco C: Comparison of clinical versus ultrasound-determined synovitis in juvenile idiopathic arthritis. *Arthritis Rheum* 2009, 61:1497–1504.

31. Haslam KE, McCann LJ, Wyatt S, Wakefield RJ: The detection of subclinical synovitis by ultrasound in oligoarticular juvenile idiopathic arthritis: a pilot study. *Rheumatology (Oxford)* 2010, 49:123–127.

32. Collado P, Jousse-Joulin S, Alcalde M, Naredo E, D'Agostino MA: Is ultrasound a validated imaging tool for the diagnosis and management of synovitis in juvenile idiopathic arthritis? A systematic literature review. *Arthritis Care Res (Hoboken)* 2012, 64:1011–1019.

33. Magni-Manzoni S, Scire CA, Ravelli A, Klersy C, Rossi S, Muratore V, Visconti C, Lanni S, Merli P, Montecucco C: Ultrasound-detected synovial abnormalities are frequent in clinically inactive juvenile idiopathic arthritis, but do not predict a flare of synovitis. *Ann Rheum Dis* 2013, 72:223–228.

34. Ikeda K, Kambe N, Satoh T, Matsue H, Nakajima H: Preferentially inflamed tendon sheaths in the swollen but not tender joints in a 5-year-old boy with Blau syndrome. *J Pediatr* 2013, 163:1525–e1521.

35. Wakefield RJ, Balint PV, Szkudlarek M, Filippucci E, Backhaus M, D'Agostino MA, Sanchez EN, Iagnocco A, Schmidt WA, Bruyn GA, Kane D, O'Connor PJ, Manger B, Joshua F, Koski J, Grassi W, Lassere MN, Swen N, Kainberger F, Klauser A, Ostergaard M, Brown AK, Machold KP, Conaghan PG: Musculoskeletal ultrasound including definitions for ultrasonographic pathology. *J Rheumatol* 2005, 32:2485–2487.

36. Ikeda K, Seto Y, Narita A, Kawakami A, Kawahito Y, Ito H, Matsushita I, Ohno S, Nishida K, Suzuki T, Kaneko A, Ogasawara M, Fukae J, Henmi M, Sumida T, Kamishima T, Koike T: Ultrasound assessment of synovial pathologic features in rheumatoid arthritis using comprehensive multi-plane images of the second metacarpophalangeal joint - Identification of the components which are reliable and influential on the global assessment of the whole joint. *Arthritis Rheumatol* 2014, 66:523–532.

37. Ikeda K, Seto Y, Ohno S, Sakamoto F, Henmi M, Fukae J, Narita A, Nakagomi D, Nakajima H, Tanimura K, Koike T: Analysis of the factors which influence the measurement of synovial power Doppler signals with semi-quantitative and quantitative measures - a pilot multicenter exercise in Japan. *Mod Rheumatol.* in press and [Epub ahead of print].

38. Iwamoto T, Ikeda K, Hosokawa J, Yamagata M, Tanaka M, Norimoto A, Sanayama Y, Nakagomi D, Takahashi K, Hirose K, Sugiyama T, Sueishi M, Nakajima H: Ultrasonographic assessment predicts relapse after discontinuation of biological agents in patients with rheumatoid arthritis in clinical remission - high predictive values of total gray-scale and power Doppler scores which represent residual synovial inflammation before discontinuation. *Arthritis Care Res.* in press and [Epub ahead of print]. doi: 10.1002/acr.22303.

39. Inoue Y, Kawaguchi Y, Shimojo N, Yamaguchi K, Morita Y, Nakano T, Arima T, Tomiita M, Kohno Y: A case of infantile Takayasu arteritis with a p.D382E NOD2 mutation: an unusual phenotype of Blau syndrome/early-onset sarcoidosis? *Mod Rheumatol* 2013, 23:837–839.

40. Schwartzman S, Fleischmann R, Morgan GJ Jr: Do anti-TNF agents have equal efficacy in patients with rheumatoid arthritis? *Arthritis Res Ther* 2004, 6:S3–S11.

41. Ikeda K, Cox S, Emery P: Aspects of early arthritis. Biological therapy in early arthritis - overtreatment or the way to go? *Arthritis Res Ther* 2007, 9:211.

42. Hayward K, Wallace CA: Recent developments in anti-rheumatic drugs in pediatrics: treatment of juvenile idiopathic arthritis. *Arthritis Res Ther* 2009, 11:216.

43. Milman N, Andersen CB, Hansen A, van Overeem Hansen T, Nielsen FC, Fledelius H, Ahrens P, Nielsen OH: Favourable effect of TNF-alpha inhibitor (infliximab) on Blau syndrome in monozygotic twins with a de novo CARD15 mutation. *APMIS* 2006, 114:912–919.

44. McGonagle D, McDermott MF: A proposed classification of the immunological diseases. *PLoS Med* 2006, 3:e297.

Scientific Research

Usefulness of a Newly-Developed Device, the Power Tree®, for Body Massage: Evidence from a Medical Evaluation

Kentaro Ishii[1], Mayumi Kotani[1], Akihito Fujita[1], Shinichi Moriwaki[2]

[1]Bloom Classic Co., Matsuyama, Japan
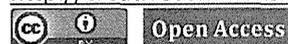[2]Department of Dermatology, Osaka Medical College, Takatsuki, Japan
Email: der002@poh.osaka-med.ac.jp

Abstract

We investigated the effectiveness and usefulness of a novel tool: the Power Tree®, for body massage in 10 healthy female volunteers (age range, 24 - 55 years; mean age, 40.5 years) by evaluating several dermatological and psychological parameters, such as the amount of dermal collagen, the skin temperature, the level of salivary amylase and the scores on the State-Trait Anxiety Index (STAI). After 60-minute Power Tree®-mediated body massage, both the dermal collagen score determined from the DermaLab® images and skin temperature measured by infrared thermography were found to have increased significantly in several body sites compared to those before the treatment ($p < 0.01$ and $p < 0.001$, respectively). Although the level of stress estimated by the amount of amylase in the saliva was not significantly different pre- and post-procedure ($p = 0.3$), the treatment significantly reduced both the state anxiety (SA) and trait anxiety (TA) scores on the STAI ($p < 0.001$ for the SA, $p < 0.01$ for the TA). The treatment with this device was smoothly performed without any burden on the therapists during the present study. These data suggest that the newly-developed device is a powerful and useful tool for reflexology when used for full body massage therapy, and massage therapy using this device may produce beneficial, physiological effects as well as psychosocial improvements.

Keywords

Dermal Collagen Score, Hand Massage, Power Tree®, Salivary Amylase, Skin Temperature, STAI

1. Introduction

There are a number of procedures used in the aesthetic and aesthetic dermatological field, where people can re-